Brazilian Journal of Chemical Engineering (2024) 41:737–751
https://doi.org/10.1007/s43153-023-00404-0

ORIGINAL PAPER

Evaluating starchy food effluents as potential green inhibitors of calcium carbonate scale in oil and gas production

Jessica Oliveira[1] · Ronald Wbeimar Pacheco Ortiz[1] · Nayanna Souza Passos[1] · Fabricio Venancio[1] · Vinicius Ottonio O. Gonçalves[1] · João Cajaiba[1] · Regiane Ribeiro-Santos[2] · Daniel Perrone[2] · Vinicius Kartnaller[1]

Received: 29 October 2022 / Revised: 29 June 2023 / Accepted: 10 September 2023 / Published online: 10 October 2023

Abstract

The development of green scale inhibitors has been the subject of several recent studies aimed at reducing the negative environmental impacts of the oil and gas industry. This work evaluated the potential of saccharides, polysaccharides, and starchy food effluents (washing wastewaters from potato, sweet potato, cassava, and potato peels) as biodegradable substances to inhibit calcium carbonate scale formation. Calcium carbonate precipitation experiments were initially conducted to assess the influence of glucose, maltose, maltodextrin, and soluble starch on the induction time, particle size, and morphology of the precipitates. The presence of these molecules resulted in a delay in the induction time of crystallization, with the delay increasing as the polymer chain size increased. Scanning electron microscopy, X-ray diffraction, and Raman spectroscopy analysis revealed that the saccharides and polysaccharides promoted the formation of calcite with an irregular shape and smaller crystallite size. The polymer chain size also affected the scaling time determined in tube blocking tests conducted in two brine scenarios (more severe and less severe), demonstrating the inhibitory potential of these molecules. However, only soluble starch proved to be effective in inhibiting scale formation in the less severe brine scenario. Based on these preliminary results, starchy food effluents were selected to evaluate their potential for inhibiting scale formation. The effluents from sweet potato and potato peels showed better performance compared to the potato effluent. The sweet potato effluent efficiently inhibited scale formation in the less severe brine scenario, possibly due to the presence of phenolic compounds and other substances, in addition to soluble starch, that also have inhibitory effects. In contrast, the cassava effluent was incompatible with the brines, leading to immediate scale formation in both scenarios.

Keywords Calcium carbonate scale · Green scale inhibitors · Tube-blocking test · Compatibility test · Polysaccharides · Food wastewater

Introduction

Scale formation is one of the main issues faced by the oil and gas industry because it can reduce productivity and consequently generates great economic losses. Scale formation occurs when inorganic salts adhere and accumulate on the internal surfaces of pipelines and can partially or totally clog them or, in worst-case scenarios, close the well (Li et al. 2017). Calcium carbonate often causes scale issues, particularly in the Brazilian pre-salt oil fields where is the most abundant inorganic salt (da Costa et al. 2016). Therefore, the oil and gas industry must implement strategies to remediate or prevent calcium carbonate scale. Acid dissolution is the main remediation strategy; however, this operation is expensive due to the production stoppage and equipment rental to perform it. Moreover, acids corrode the pipes and their improper disposal can be polluting (Kamal et al. 2018).

Chemical products known as scale inhibitors are the current strategy used by the oil and gas industry to prevent scale. These chemicals influence different stages of calcium carbonate scale formation, including nucleation,

✉ Vinicius Kartnaller
kartnaller@iq.ufrj.br

[1] Instituto de Química, NQTR – Núcleo de Desenvolvimento de Processos e Análises Químicas em Tempo Real, Universidade Federal do Rio de Janeiro, Rua Hélio de Almeida, 40, Cidade Universitária, Rio de Janeiro 21941-614, RJ, Brazil

[2] Instituto de Química, Laboratório de Bioquímica Nutricional e de Alimentos, Universidade Federal do Rio de Janeiro, Av. Athos da Silveira Ramos 149, CT, Bloco A, sala 528 A, Rio de Janeiro 21941-909, Brazil

crystallization, and crystal growth, preventing the accumulation and formation of deposits or promoting the formation of weak deposits. Phosphorous compounds are common chemicals used as scale inhibitors because of their high efficiency and high resistance to the conditions (*e.g.* high temperature and high pressure) where scale occurs. Organophosphate compounds, such as phosphate esters, are chemical inhibitors extensively used. These chemicals can withstand temperatures higher than 80 ºC. Other phosphorous chemical inhibitors are aminophosphonates, being the diet hylenetriaminepenta(methylenephosphonic) acid (DTPMP) the most used. Polymeric type inhibitors are also used by the petroleum industry, including phosphinopolycarboxylic acid (PPCA), polyacrylates, polyphosphinocarboxylates, polymaleates and polyvinyls. The polymeric inhibitors are stable up to of 200 ºC (Jensen and Kelland 2012; Li et al. 2017; Kumar et al. 2018). However, as the chemical inhibitor in general are very stable compounds, they are also associated with environmental issues as their improper disposal can cause the eutrophication of aquatic ecosystems (Hasson et al. 2011; Jafar Mazumder 2020). In this regard, research on biodegradable molecules efficient in inhibiting scale is important aiming to reduce the negative environmental impacts of the oil and gas industry. Thus, the development of green scale inhibitors has been the subject of several recent studies (Martinod et al. 2009; Elkholy et al. 2018; Macedo et al. 2019; Wang et al. 2021).

Green scale inhibitors must be non-toxic, non-bioaccumulative, and biodegradable (Martinod et al. 2009; Hasson et al. 2011). Research has focused on the development of biodegradable polymers that can also influence the mechanisms of nucleation and crystallization of calcium carbonate. These biopolymers have been extensively applied as scale inhibitors to meet the criteria for environmentally friendly inhibitors (Macedo et al. 2019). These biopolymers or biomolecules are naturally occurring substances involved in biomineralization processes, where they play a crucial role in influencing the size, morphology, and crystallographic orientation of structures formed by living organisms (Manoli and Dalas 2000; Meldrum 2003; Rao et al. 2014). The influence of these biopolymers on calcium carbonate arises from the presence of specific functional groups in their structures, such as carboxyl and hydroxyl groups, which contribute to chelation, dispersion, and crystal distortion effects (Macedo et al. 2019).

There are many sources of biopolymers such as plants, algae, fungi, bacteria, and animals (Zakyatul et al. 2022). Cellulose, hemicellulose, chitin, inulin, lignin, and starch are examples of biopolymers of saccharides (polysaccharides) with variable molar mass. A saccharide is a molecule that contains mainly a functional group aldehyde or ketone within a polyhydroxylated chain (Reis et al. 2011b). Polysaccharides comprise approximately 75% of earth's biomass and are a large renewable source of biopolymers and therefore, a potential source of green scale inhibitors. Moreover, polysaccharides such as starch are the main source of human nutrition. Therefore, byproducts and effluents from industrial processing of starchy foods can be an abundant and inexpensive source of biopolymers or other molecules whose feasibility as green scale inhibitors can be evaluated (Ferreira et al. 2009). The use of starchy food effluent to prevent the calcium carbonate scale could be an environmentally friendly strategy for the oil and gas industry to manage this flow assurance issue.

This work evaluates the influence of a series of model saccharides (glucose and maltose) and polysaccharides (maltodextrin and soluble starch) and starchy food effluents (washing wastewater of potato, sweet potato, cassava, and potato peels) on the calcium carbonate scale formation. Precipitation experiments of calcium carbonate in the presence of the model molecules were performed to observe their effect on particle size and morphology, which in turn aid to understand their effect on scale formation under flow conditions. Moreover, several tube-blocking tests were performed in a dynamic scale system (DSL) to evaluate the potential of the saccharides and starchy food effluents to inhibit calcium carbonate scale.

Experimental

Reagents and standards

This work evaluates saccharides that can be found in starchy foods and their byproducts and effluents: glucose, maltose, maltodextrin, and soluble starch. They were analytical grade and purchased from ACS Cientifica (Sumare, Brazil). Additionally, calcium chloride, sodium bicarbonate, and sodium chloride purchased from Isofar (Rio de Janeiro, Brazil) were used to prepare the brine.

The starchy effluents were characterized using the following standards: 5-caffeoylquinic acid (chlorogenic acid, 5-CQA), 3,4-dihydroxybenzoic acid, and ferulic acid, all of which were purchased from Sigma-Aldrich. High-performance liquid chromatography (HPLC)-grade solvents from Tedia (Fairfield, OH, USA) were used, and HPLC-grade water from the Milli-Q system (Millipore, Bedford, MA, USA) was employed in the experiments.

Preparation of the brines

The calcium chloride and sodium bicarbonate solutions were prepared with degassed ultrapure water. The salinity of both solutions was adjusted by adding sodium chloride to obtain a final concentration of 35,000 mg L^{-1} of total chloride. The pH of the solutions was adjusted to 7.0 by adding

hydrochloric acid or sodium hydroxide to the calcium chloride solution and by bubbling CO_2 into the sodium bicarbonate solution. After the solutions mix, the final composition was as presented in Table 1.

Precipitation experiments

.

Preliminary experiments were performed to assess the precipitation of calcium carbonate in the presence of the model saccharides and polysaccharides in 1000 mg L^{-1}. They were performed in an Easymax 102 workstation from Mettler Toledo (Greinfensee, Switzerland). The 100 mL reactor vessel was set at 30 °C with magnetic stirring at 200 rpm. The bicarbonate solution containing the model molecule was mixed with the calcium chloride solution to obtain the final concentration of Brine 1 (Table 1). Then, the precipitation of calcium carbonate was followed through RGB (red, green, and blue) image analysis using a webcam (Microsoft LifeCam) and the software RGBview® (developed by our research group). Additionally, the pH was continuously measured using a SeveMulti pH-meter (Mettler Toledo). After detecting the precipitation through the increase of RGB signal and decrease of pH, the system was left under these experimental conditions for 1 h. Then, the solids were recovered by vacuum filtering, washing with ethanol, and drying at 50 °C for 1 h.

Characterization of calcium carbonate solids formed in the presence of model molecules

The solids recovered were characterized with scanning electron microscopy (SEM), X-ray powder diffraction (XRD), and Raman spectroscopy analysis.

The surface microstructure (*i.e.*, morphology and particle size) of the samples were characterized using SEM on a ZEISS EVO10 microscope (Oberkoshen, Germany). Each powdered sample was placed on a conducting carbon pad (Plano GmbH) and coated with a thin gold layer. Beam scan mapping was performed at 15 kV acceleration voltage.

The crystalline structure of the samples was determined by XRD using a PANalytical AERIS X-ray diffractometer (Malvern, UK) with Ni-filtered\Cu$K_\alpha$ radiation (k = 1.5406 Å) generated at 40 kV and 30 mA. The XRD patterns were collected in a Bragg angle (2θ) range of 5−90° with a step size of 0.002° in continuous mode and a counting time of 8.670 s per step. Crystalline phases were qualitatively identified using the MDI Jade v.5.0.37 (SP1) software (International Center for Diffraction Data, USA) by matching the XRD patterns against the JCPDS (Joint Committee on Powder Diffraction Standards) database.

Raman spectra were acquired using an Anton-Paar Cora 5000 Raman spectrometer (Graz, Austria) equipped with two laser excitations (1064 and 785 nm). The 784 nm laser was chosen to minimize potential sample fluorescence. The measurements were performed at 150 mW of laser power and an exposure time of 5000 ms.

Table 1 Composition of the different brines used in this study

	$[Ca^{2+}]$ (mg L^{-1})	$[HCO_3^-]$ (mg L^{-1})
Brine 1	1,080	2,180
Brine 2	540	1,090

Preparation of the starchy food effluents

The starchy foods selected to evaluate the potential of their effluents as green scale inhibitors were potato, sweet potato, and cassava. The effluent used was the washing wastewater of their pulps and additionally the washing wastewater of the peels of both potatoes (potato and sweet potato). These effluents were produced by peeling the starchy foods and slicing them into approximately 1–2 cm^3 pieces. The starchy foods pieces were submerged in distilled water (500 g per liter of water) overnight. The residual waters (Fig. 1) were vacuum filtered through cotton to separate larger residues and then freeze-dried. The freeze-dried starchy food effluents were later re-dissolved to HPLC analysis and to prepare a stock solution of 4000 mg L^{-1} that was stored under refrigeration until used in the tube-blocking tests.

Tube-blocking tests

The method for the tube-blocking tests performed in this study is based on the NACE 31,105 standard (da Rosa et al. 2020). This test evaluates the inhibition efficiency of a chemical, which in this study were the model saccharides and polysaccharides and the starchy food effluents. The tube-blocking tests are performed in a dynamic scale loop (DSL) equipment (Fig. 2). The DSL has two high-pressure pumps PU-4087 from Jasco (Tokyo, Japan) to pump the solutions that compose the brine (Table 1) through individual stainless-steel coils (Coil 1 and Coil 2) with an internal diameter of 1 mm and a length of 1 m. The coils are located inside an oven set at the experimental temperature to condition the solutions prior to mixing. The solutions mix inside a coil (test coil) with internal diameter of 0.5 mm and a length of 1 m, which is also located inside the oven. A pressure transducer detects the scale formation when the differential pressure between the inlet and outlet of the test coil increases.

The response obtained in the tube-blocking test is the scaling time, which is the time that elapses between the mixing of the solutions and the initiation of the differential

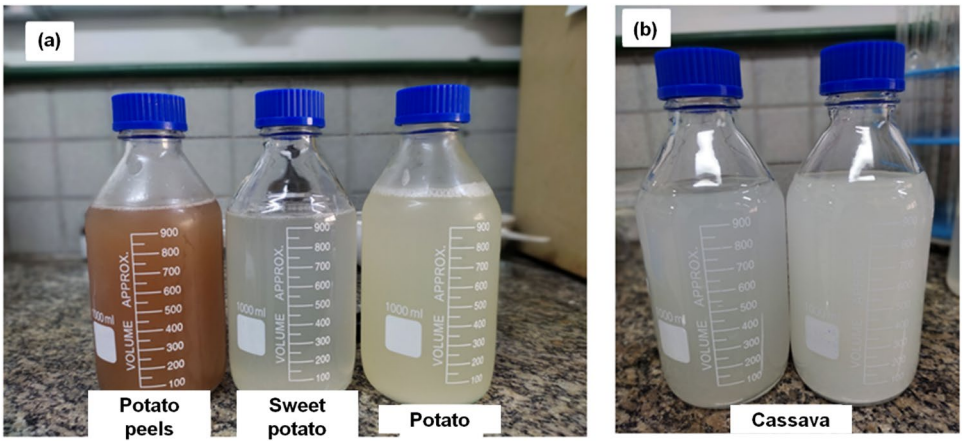

Fig. 1 Starchy food effluents. **a** Potato peels (potato and sweet potato peels), sweet potato and potato, and **b** cassava

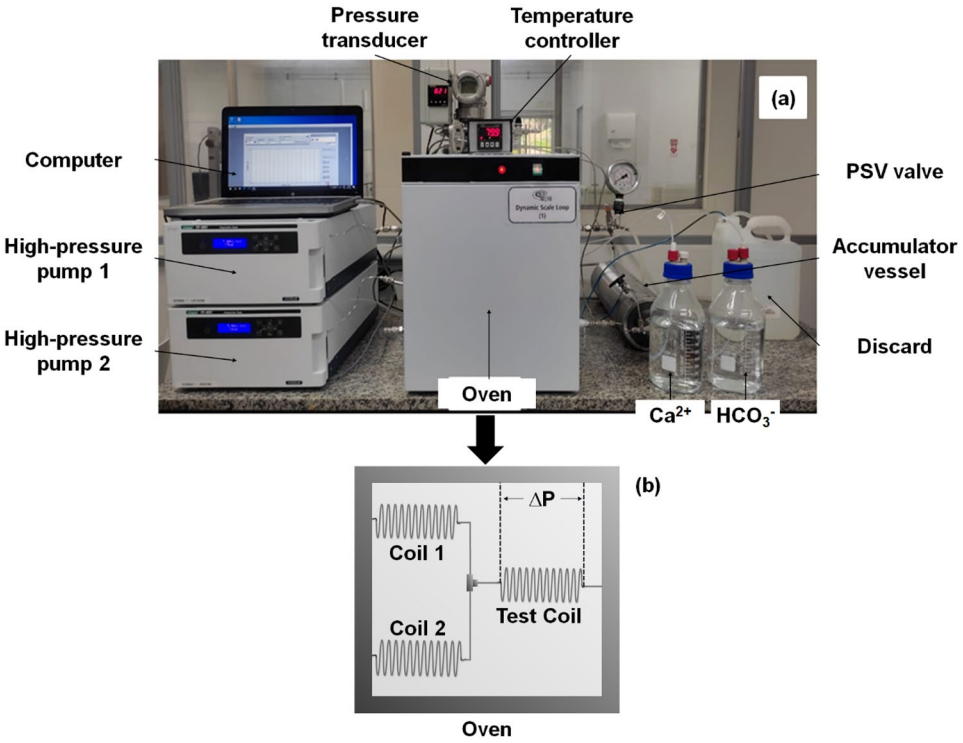

Fig. 2 Dynamic scale loop equipment. **a** Picture of the dynamic scale loop, and **b** Schematic of the oven interior

pressure increase. A control experiment (blank) performed without the addition of the chemical (scale inhibitor) defines 4-psi as the increase of the differential pressure that occurs when the scale forms. An effective scale inhibitor must not exceed a differential pressure of 0.5-psi for a time equivalent to threefold the scaling time of the blank or a total time of 1 h, whichever is the longest. The experimental conditions for the tube-blocking tests were a continuous flow of 5 mL min^{-1} for each solution, pumping pressure of 10 bar, and 80 °C. The model molecules and the starchy food effluents were added to the sodium bicarbonate solution in concentrations ranging from 50 to 1000 mg L^{-1}.

Compatibility tests

The compatibility tests were conducted using the two brines described in Table 1. The solutions were adjusted to a salinity of 35,000 mg L^{-1} and pH 7.0. For the anion solution, sodium bicarbonate was excluded and replaced with NaCl to maintain the original solution's ionic strength. The starchy food effluents were added to the anion solution at concentrations ranging from 50 to 1000 mg L^{-1}. Separate 25 ml bottles were used for the cation and anion solutions. These bottles were then placed in an oven and heated to 80ºC for 1 h. Subsequently, the solutions were mixed, and the turbidity of the mixture was measured after 1 and 24 h. Additionally, images of the solutions were captured for further analysis.

Characterization of the starchy food effluents

The starchy food effluents were characterized using Fourier transform infrared spectroscopy (FTIR) and high-performance liquid chromatography with a diode array detector (HPLC-DAD).

For the FTIR analysis, infrared spectra was acquired using a Thermo Scientific Nicolet 6700 instrument. The following specifications were used for the middle infrared region (MID): 16 scans, DTGS-KBr detector, KBr beamsplitter, and analysis in the range of 4000 cm $^{-1}$ to 400 cm $^{-1}$, with 4 cm $^{-1}$ resolution. The analysis was performed by transmission, and the sample preparation technique involved pressing a mixture of the sample with potassium bromide (KBr) to form a tablet for reading.

Phenolic compounds in the starchy food effluents were analyzed using HPLC-DAD. Prior to analysis, all freeze-dried samples were re-dissolved in purified water, homogenized, and filtered through a 0.45 µm SFPTFE filter unit (Millipore, Barueri, Brazil). The liquid chromatography system (Shimadzu®, Japan) consisted of a quaternary pump LC-20AT, a manual injector 7725 (Rheodyne) with a 20 µL loop, a diode array detector SPD-M20A, a system controller CBM-20 A, and a degasser DGU-20A5. A C18 column (5 µm, 250 mm x 4.6 mm, Phenomenex®) was used for chromatographic separations, and gradient elution was employed (Alves and Perrone, 2015). The mobile phase consisted of a gradient of water with 0.3% formic acid and 1% acetonitrile (eluent A) and 1% acetonitrile in methanol (eluent B) with a constant flow rate of 1.0 mL/min. The column was equilibrated with 18.2% B prior to sample injection. After injection, the proportion of eluent B was increased to 20.2% in 1 min, 43.4% in 18 min, and 85.9% in 23 min, and then kept constant up to 30 min. A 10-min interval was used between injections to re-equilibrate the column with 18.2% B. Phenolic compounds were monitored by DAD in the wavelength range of 260 to 325 nm. The identification of specific compounds such as 5-caffeoylquinic acid (5-CQA), 3,4-dihydroxybenzoic acid, and ferulic acid was performed by comparing their retention times and UV spectra with those of commercial standards. Additionally, small amounts of the appropriate standards were spiked into the samples for confirmation. The identification of other compounds such as 3,4-dicaffeoylquinic acid (3,4-diCQA), 3,5-dicaffeoylquinic acid (3,5-diCQA), 4,5-dicaffeoylquinic acid (4,5-diCQA), and 4-feruloylquinic acid (4-FQA) was based on comparing their retention times and UV spectra with those of chlorogenic acids (CGAs) from green coffee, as previously studied. Quantification of 5-CQA, 3,4-dihydroxybenzoic acid, and ferulic acid was performed by external standardization. The quantification of 3,4-diCQA, 3,5-diCQA, 4,5-diCQA, and 4-FQA was carried out using the area of the 5-CQA standard combined with the molar extinction coefficients of the respective chlorogenic acids (Trugo and Macrae, 1984). The data were acquired using LC solution software (Shimadzu Corporation, version 1.23), and the results were expressed as mg of compound per 100 g.

Results and discussion

This work evaluates the influence of four model molecules on calcium carbonate scale, a monosaccharide (glucose), a disaccharide (maltose), and two polysaccharides (maltodextrin and soluble starch). The structures of these molecules contain hydroxyl groups whose amount varies according to the polymer chain size (Fig. 3). Previous works had already tested hydroxylated molecules such as monoethylene glycol as calcium carbonate scale inhibitors, showing their good performance (Kartnaller et al. 2018; Venancio et al. 2018). The evaluation of the four model molecules selected in this study reveals the effect of the polymer chain size (*i.e.* the number of hydroxyl groups) on calcium carbonate scale. Moreover, these molecules occur in starchy foods, and therefore, these results aid to understand the influence of starchy food effluents on calcium carbonate scale.

The precipitation of calcium carbonate in the presence of the model molecules was performed to evaluate the effects on the induction time, particle size and morphology, and crystalline structure of the precipitates. Figure 4a shows the induction time of the calcium carbonate precipitation in the presence of the model molecules, which was determined through RGB image analysis and pH measurement. The presence of all model molecules prolongs the induction time compared to blank test, showing a slight effect on precipitation kinetics. Moreover, the induction time increases with the increase in polymer chain size, suggesting that a greater number of hydroxyl groups promotes a greater interaction

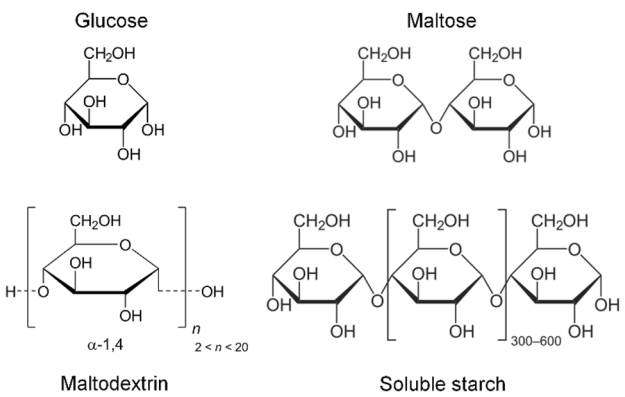

Fig. 3 Chemical structure of the model molecules evaluated in this study. Monosaccharide: glucose, disaccharide: maltose, and polysaccharides: maltodextrin and soluble starch

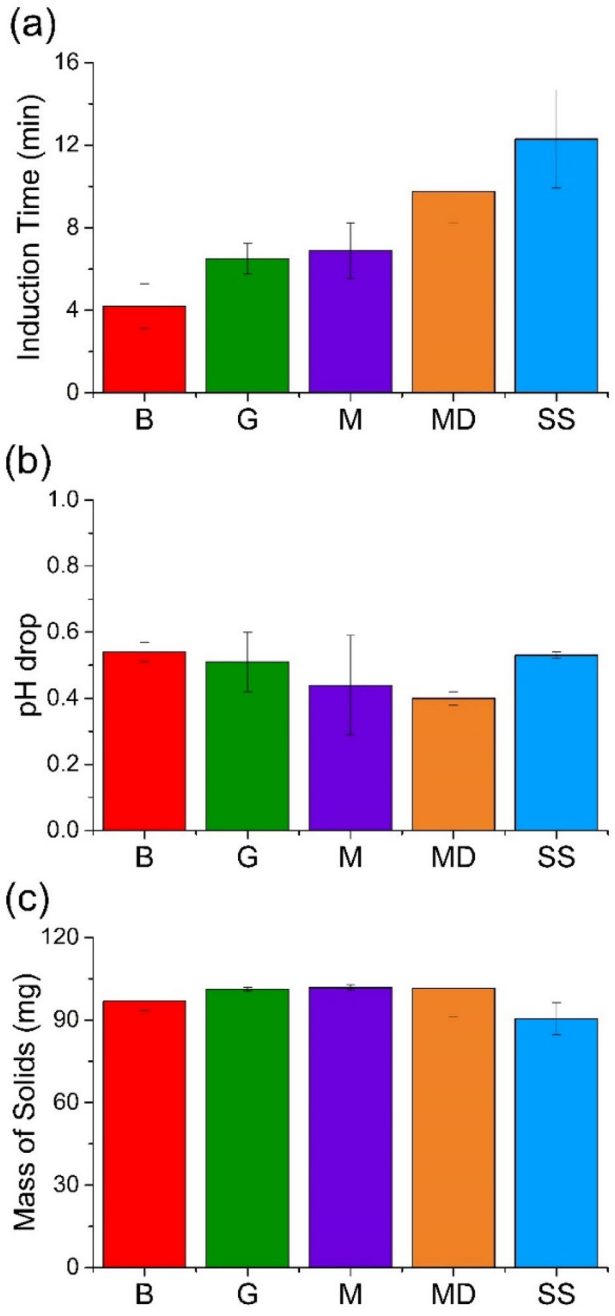

Fig. 4 Calcium carbonate precipitation, in brine 1, temperature of 30º C in the presence of the model saccharides and polysaccharides at 1000 mg L^{-1}. **a** Induction time, **b** pH drop, and **c** mass of solids recovered. B: Blank, G: Glucose, M: Maltose, MD: Maltodextrin, and SS: Soluble Starch

with the precipitant ions delaying the nucleation or modifying its mechanism.

(Rao et al. 2014) have already described the effects of glucose and maltose on calcium carbonate nucleation. These authors report that glucose (and derived molecules) inhibits nucleation whereas maltose destabilizes pre-nucleation clusters. Moreover, the impact of the size of the polymer chain may be due to the nature of calcium carbonate nucleation itself. As has been deeply debated and studied in the past decade, calcium carbonate does not follow the classical nucleation theory, but a non-classical one, where the mechanism for its formation has a liquid-liquid phase transition. As calcium and carbonate ion aggregates forming pre-nucleation clusters, a liquid-liquid binodal can be reached, where nanodroplets of a new liquid phase form, that may later aggregate and go through solvent loss to form a new solid phase, leading to the crystallization. This liquid precursor of the nucleation and its stability can be deeply related to the presence of other ions and molecules in solutions, and several studies have shown the impact of polyelectrolytes compounds on its stabilization. Studies have shown that acidic polypeptides, such as poly(aspartic acid), may induce the formation of a polymer induced liquid precursor (PILP) (Schenk et al. 2012). Furthermore, the work has also shown that poly(aspartic acid) and poly(acrylic acid) seem to stabilize the colloidal liquid nanodroplets against aggregation and or/prevent the solvent loss, thus inhibiting the crystallization (Sebastiani et al. 2017). Even though the polysaccharides do not have acidic groups (but rather hydroxyl ones), results show that this polymeric effect still influences calcium carbonate crystallization. Rather the mechanism might be different to the polycarboxylates, the polysaccharides might still be influencing the pre-nucleation phase of calcium carbonate crystallization and further studies may indicate the correct mechanism. It is important to note that different heteroatoms with non-binding electrons have the potential to interact with calcium and other divalent cations, which can potentially influence the crystallization process. However, the specific way in which these interactions relate to non-classical nucleation remains an aspect that requires further investigation and clarification.

However, Fig. 4b displays the pH drop at the initiation of calcium carbonate precipitation, which was similar in the presence of all model molecules. The drop in pH is due to the hydronium ions produced as the calcium carbonate precipitates according to Eqs. (1) and (2). Therefore, this drop indicates indirectly that the amount of calcium carbonate precipitated is also similar in the presence of all model molecules.

$$HCO^{-}_{3(aq)} + H_2O_{(l)} \rightleftharpoons CO^{2-}_{3} + H_3O^{+}_{(aq)} \quad (1)$$

$$CO^{2-}_{3(aq)} + Ca^{2+}_{(aq)} \rightleftharpoons CaCO_{3(s)} \quad (2)$$

The latter was corroborated by the similar mass of solids recovered from the precipitation experiments shown in Fig. 4c. This finding suggests that the model molecules evaluated influence nucleation kinetics but do not influence

precipitation equilibrium. Moreover, Figs. 5 and 6; Table 2 presents the effects of these molecules on the particle size, morphology, crystalline structure, and crystallite size. Figure 5 displays the SEM images of the solids formed in the presence of the model molecules.

Calcium carbonate particles exhibit a typical calcite morphology in all the samples, including the blank experiment. The SEM images confirm that the tested model molecules do not significantly influence the precipitation equilibrium, as the morphology and size of the particles are similar to those in the blank test. The formation of calcite was check with XRD and Raman spectroscopy analysis. Figure 6a shows the XRD patterns of the precipitates, which are the same for all the samples and are typical of crystalline rhombohedral (R-3c) calcite phase. Raman spectroscopy also confirms the formation of calcite phase as the spectra show the major bands attributed to calcite: 1086 and 711 cm^{-1}, corresponding to the symmetric (ν_1) stretching modes and the in-plane bending (ν_4), respectively.

Moreover, the model saccharides and polysaccharides influence the crystallite size. Table 2 presents the crystallite sized calculated from the XRD patterns using the Scherrer equation (Patterson 1939) that relates this parameter with the full width at half-maximum intensity of the XRD reflections. Table 2 shows that the presence of the model saccharides and polysaccharides reduces the crystallite size. Soluble starch was the molecule that reduces the crystallite size the most. This is an interesting result that suggests that this effect may be also related to the greater number of hydroxyl groups. However, there is not sufficient information to conclude this, as the glucose reduces the crystallite size more than maltose and maltodextrin, even though it has fewer hydroxyl groups.

The potential of the model saccharides and polysaccharides to inhibit calcium carbonate scale was then evaluated by performing several tube-blocking tests in two scenarios regarding the concentration of the precipitant ions (Table 1). Figure 7a show that the scaling time of the blank test for the brine 1 is 2 min and 42 s. The brine 1 is a severe condition (high concentration of precipitant ions) for the formation of calcium carbonate scale hence the increase of the differential pressure occurs rapidly. In this condition, the soluble starch is the molecule that delays the scaling time the most, followed by the maltodextrin and maltose. Although these three molecules only slightly delay the scaling time, this result suggests its potential inhibitory effect. However, glucose, the only monosaccharide evaluated, does not show any effect as its scaling time is similar to the blank experiment. Despite the delay of the scaling time promoted by the addition of 1000 mg L^{-1} of soluble starch, maltodextrin, and maltose,

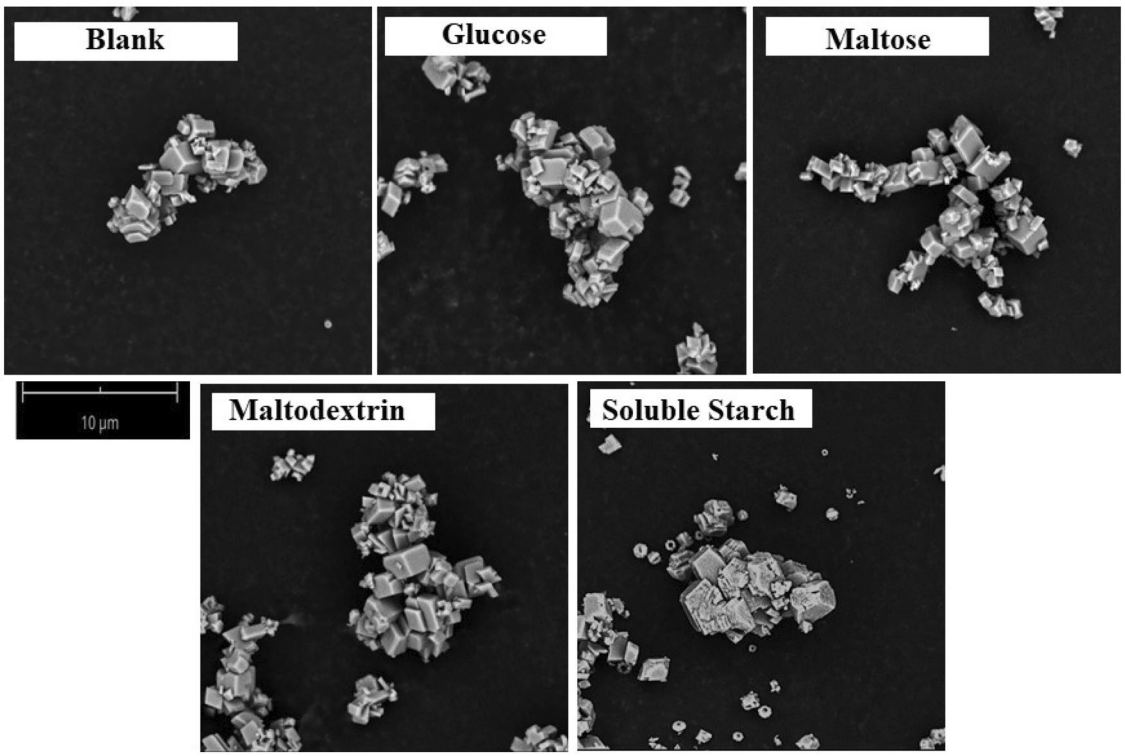

Fig. 5 SEM images of calcium carbonate precipitates formed in the presence of different model saccharides and polysaccharides. Magnification: 6000X

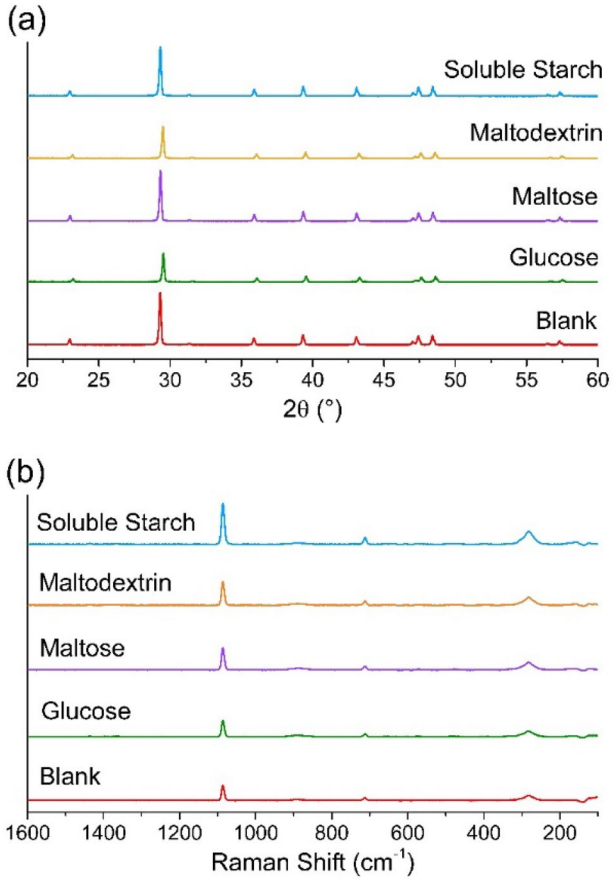

Fig. 6 XRD patterns and Raman spectra of calcium carbonate precipitates formed in the presence of different model saccharides and polysaccharides. **a** XRD patterns and **b** Raman spectra

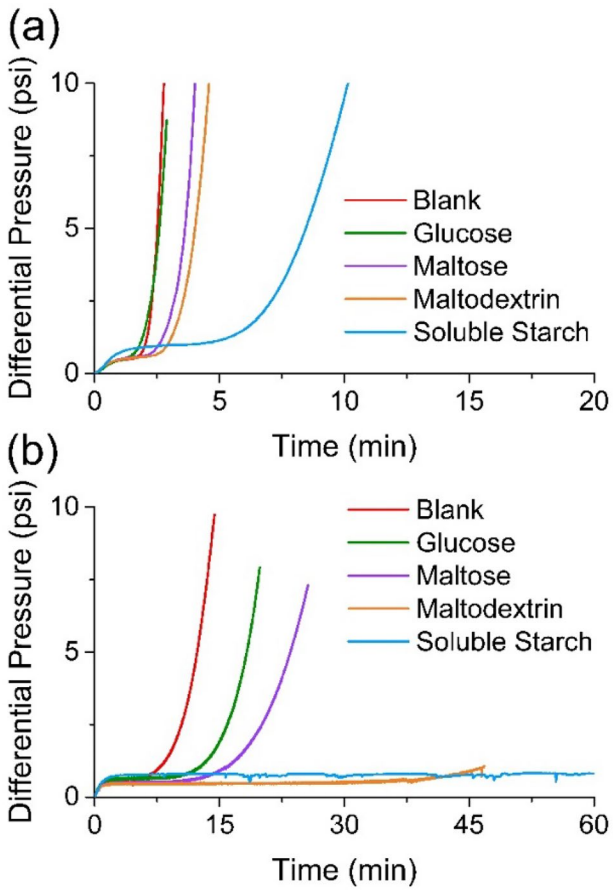

Fig. 7 Evaluation of model saccharides and polysaccharides to inhibit calcium carbonate scale in two brine scenarios at 80 ºC. **a** Brine 1 and **b** Brine 2. The concentration of the model molecules was 1000 mg L^{-1}

Table 2 Crystallite size of the calcite formed in de presence of the model saccharides and polysaccharides

Molecule	Crystallite size (nm)
Blank	317
Glucose	223
Maltose	281
Maltodextrin	274
Soluble starch	190

according to the NACE 31,105 standard procedure (da Rosa et al. 2020), none of these molecules is efficient in inhibiting calcium carbonate scale in this brine scenario.

The brine 2 has a lower concentration of precipitant ions than brine 1 and therefore is a less severe condition for calcium carbonate scale formation, resulting in a scaling time of 8 min and 16 s for the blank. The model molecules show a greater inhibitory effect for the brine 2 compared to the brine 1 as shown in Fig. 7. The slight inhibitory effect observed in Fig. 7 of the model molecules may be related to their effect on the induction time of the calcium carbonate precipitation (Fig. 4). Soluble starch is the molecule that delays the scaling time the most followed by maltodextrin, maltose, and glucose. This result suggests that the greater the size of the polymer chain, the greater the inhibitory effect. Soluble starch, a long-chain polysaccharide composed of more than 200 glucose monomers (Fig. 3), shows a greater inhibitory effect than maltodextrin, which is a polysaccharide composed of up to 20 glucose monomers. Maltose, composed of two glucose monomers, and the glucose itself, do not show a considerable inhibitory effect for both brine scenarios. (Bisatto et al. 2022) affirms that the molar mass of a polymer has a strong influence on scale inhibition efficiency. According to these authors, the increase in molar mass increases the efficiency of a molecule because of likely greater adsorption on crystalline surfaces, which induces the formation of irregular particles with non-crystalline shapes. The SEM image of the calcium carbonate precipitates formed in the presence of soluble starch show some irregular shapes (Fig. 5); however, the Raman spectrum do not show non-crystalline phases (amorphous phases) (Fig. 6).

Moreover, soluble starch does not present variations in the differential pressure greater than 0.5 psi for 1 h. Therefore, soluble starch at a concentration of 1,000 mg L^{-1} is efficient to inhibit calcium carbonate scale in the brine 2 scenario. The concentration of 1000 mg L^{-1} is higher than concentrations used for commercial scale inhibitors (e.g. phosphorous compounds); however, as the molecules used in this study are biodegradable and low cost, this concentration is a suitable starting point to evaluate their efficiency. Figure 8 shows the results of evaluating soluble starch at different concentrations ranging from 50 to 1000 mg L^{-1} to establish its minimum inhibitory concentration (MIC).

Figure 8 shows that concentrations of 500 and 1000 mg L^{-1} of soluble starch are efficient to inhibit calcium carbonate scale as the differential pressure only varies 0.34 and 0.02 psi respectively. However, the experiments with concentrations less than 500 mg L^{-1} exceed 4 psi, indicating the scale formation in less than 1 h. Therefore, the MIC of the soluble starch is 500 mg L^{-1} for the brine 2 scenario.

The performance of the soluble starch indicates that starchy food effluents may also be efficient to inhibit calcium carbonate scale because soluble starch is their main component. Soluble starch is for instance one of the main polysaccharides recovered from effluents of potato processing for applications not only in the food industry but also in other industries as in this study (Bergel et al. 2018). Starchy food byproducts and effluents such as the liquid waste from the manufacture of cassava starch and sweet potato peels are often an environmental issue (Anastácio et al. 2016; Costa et al. 2021). Therefore, much research has focused on the recovery and use of substances of commercial interest from these residues (Mironescu 2011; Torres and Domínguez 2020). Our study used potato, sweet potato, cassava, and potato peels as the source of the starchy food effluents evaluated as potential green inhibitors of calcium carbonate scale. The products obtained from the freeze-drying of the washing wastewaters of these starchy foods were tested in the two brine scenarios at a concentration of 500 mg L^{-1} and the results are presented in Fig. 9.

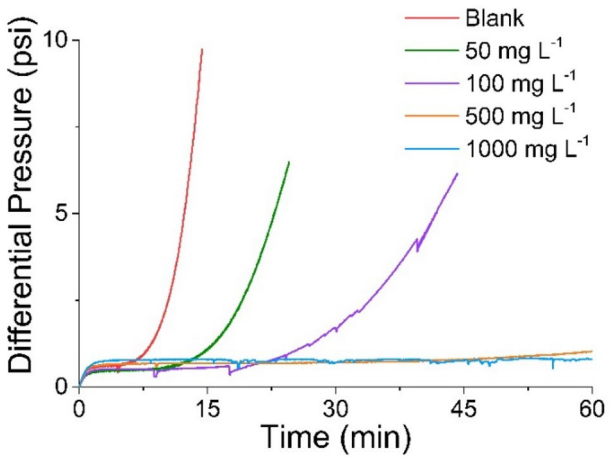

Fig. 8 Evaluation of different concentrations of soluble starch to inhibit calcium carbonate scale for brine 2 at 80 ºC

Figure 9 shows that the starchy food effluents influence the calcium carbonate scale formation even in the more severe condition of the brine 1. They also delay the scaling time more than the soluble starch at a concentration of 1000 mg L^{-1}, which is 5 min and 46 s (Fig. 7a), a shorter value than, for example, the 20 min of the potato effluent. This result is probably due to the presence of other substances rather than soluble starch in the effluents, which can also contribute to the inhibition of calcium carbonate scale (Mironescu 2011). Moreover, potato peels effluent shows a better performance than soluble starch under the test conditions, but it is not sufficient to be considered as an efficient inhibitor.

In the less severe condition, the brine 2, sweet potato was the starchy food effluent that shows the best performance. The differential pressure of the experiment with the addition

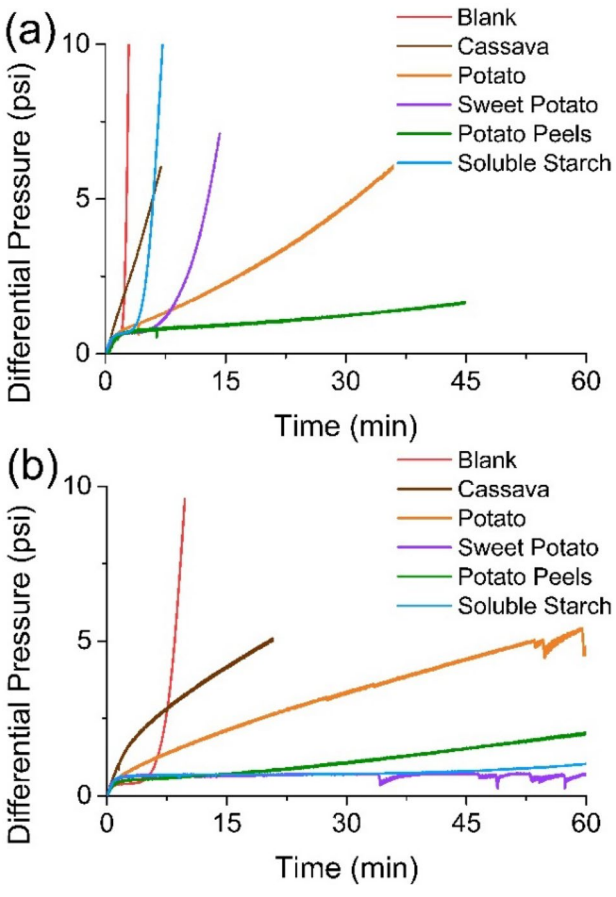

Fig. 9 Evaluation of starchy food effluents at a concentration of 500 mg L^{-1} to inhibit calcium carbonate scale. **a** Brine 1 and **b** Brine 2

of sweet potato effluent did not present variations greater than 0.05 psi for 60 min. This was a smaller increase compared to the soluble starch for the same scenario, which was 0.34 psi. Thus, according to the procedure to evaluate the inhibition efficiency, both the sweet potato effluent and the soluble starch at a concentration of 500 mg L^{-1} were efficient to inhibit calcium carbonate scale but the sweet potato effluent showed a better performance. Potato peels also showed a relevant result in this brine scenario as the differential pressure increased 0.5 psi only after 29 min; however, this time is not sufficient to consider this effluent as efficient.

Compatibility tests were also conducted using potato, sweet potato, potato peels, and cassava to assess their ability to remain soluble in the presence of Ca^{2+} ions at a specific temperature. The compatibility was determined by visually assessing each sample using a turbidimeter after 1 and 24 h. The product is considered approved if it meets the following criteria: a visibly clear solution, turbidity levels lower than 10 NTU after 24 h, and no precipitate formation after 24 h. An increase in turbidity exceeding 10 NTU or the presence of precipitation indicates a dosage limitation of the inhibitor under the tested conditions (da Rosa et al. 2020). Tables 3 and 4 present the turbidity results for different dosages of starchy food effluents added to brine 1 and brine 2, respectively.

According to Table 3, the dosage limits for brine 1 are 100 mg L^{-1} for potato, sweet potato and cassava, and 50 mg L^{-1} for the potato peels. These results indicate that all starchy effluents are incompatible at a dosage of 500 mg L^{-1} after 24 h. However, after 1 h, only the cassava effluent was incompatible. Since all solutions were freshly mixed with the brines at the time of the tube blocking test, it is unlikely that the solutions were already incompatible during the experiment. This was true except for the cassava effluent, which could explain why its scaling time was smaller than the blank experiment. The incompatibility suggests that a component of the inhibitor (in this case, the effluent) is precipitating with the brine. The presence of a precipitate in the solution may influence the nucleation step of crystallization, leading to secondary nucleation and increased solid formation kinetics. This could explain why the differential pressure for the cassava effluent increased more rapidly and linearly during the experiment. The reason why cassava exhibits this behavior more prominently may be related to the type of starch extracted from the product. Cassava typically has a higher ratio of amylopectin to amylose compared to other root and tuber crops (Moorthy 2002). The amylopectin content in starch is usually associated with its crystallinity, with branched molecules forming tightly packed double helices that are resistant to water uptake and swelling. In contrast, the linear molecules of amylose can form hydrogen bonds with water molecules, making it more soluble (MacNeill et al. 2017). The packing arrangement of amylopectin can result in different types of crystalline structures, which in turn affects overall solubility. Literature reports suggest that cassava starch exhibits A-type amylopectin crystallinity, which corresponds to a denser and more compact structure that tends to be less soluble. In contrast, potato starch exhibits B-type crystallinity, which is less dense and more hydrated, and sweet potato starch can exhibit A-, B-, or C-type crystallinity (Wang et al. 2017). Therefore, cassava starch has a greater tendency to be less soluble, leading to the precipitation of the amylopectin component of the extracted starches in the brines at a faster rate, resulting in incompatibility observed at the 1-hour mark.

For the brine 2 (Table 4), the dosage limits after 24 h were 100 mg/L for potato and cassava, 50 mg/L for potato peels, and 500 mg/L for sweet potato. Therefore, sweet potato was found to be compatible with brine 2 at a concentration of 500 mg/L, while the other starchy effluents were

Table 3 Compatibility tests for brine 1 at 80 ºC

	Potato		Sweet potato		Potato Peel		Cassava	
Dosage	Turbidity (NTU)		Turbidity (NTU)		Turbidity (NTU)		Turbidity (NTU)	
mg L^{-1}	1 hour	24hours	1 hour	24hours	1 hour	24hours	1 hour	24hours
Blank	< 10	< 10	< 10	< 10	< 10	< 10	< 10	< 10
50	< 10	< 10	< 10	< 10	< 10	< 10	< 10	< 10
100	< 10	< 10	< 10	< 10	< 10	> 10	< 10	< 10
500	< 10	> 10	< 10	> 10	< 10	> 10	> 10	> 10
1000	> 10	> 10	< 10	> 10	> 10	> 10	> 10	> 10
Caption:	Clear	Turbid < 10 NTU	Turbid > 10 NTU	Precipitate				

Table 4 Compatibility test for Brine 2 at 80 ºC

	Potato		Sweet potato		Potato Peel		Cassava	
Dosage	Turbidity (NTU)		Turbidity (NTU)		Turbidity (NTU)		Turbidity (NTU)	
mg L^{-1}	1 hour	24hours	1 hour	24hours	1 hour	24hours	1 hour	24hours
Blank	< 10	< 10	< 10	< 10	< 10	< 10	< 10	< 10
50	< 10	< 10	< 10	< 10	< 10	< 10	< 10	< 10
100	< 10	< 10	< 10	< 10	< 10	= 10	< 10	< 10
500	< 10	> 10	< 10	< 10	< 10	> 10	> 10	> 10
1000	> 10	> 10	< 10	> 10	> 10	> 10	> 10	> 10
Caption:	Clear	Turbid < 10 NTU	Turbid > 10 NTU	Precipitate				

incompatible at this concentration. Furthermore, in addition to being compatible at a dosage of 500 mg/L, sweet potato also exhibited the best performance in the tube blocking test at the same dosage. These results suggest that the sweet potato effluent holds promise as a green scale inhibitor and warrants further investigation and improvement. Regarding the 1-hour limit of the compatibility test, the cassava effluent once again demonstrated incompatibility with the brine and exhibited a faster increase in differential pressure compared to the blank experiment. However, the potato peels effluent was also incompatible with the brine but did not exhibit the same behavior. Instead, it prevented scale formation for almost 15 min. This indicates that compatibility tests need to be carefully evaluated when selecting an inhibitor since they can operate through various mechanisms. An inhibitor may not prevent precipitation or may even induce precipitation and still function effectively, as demonstrated by the potato peels. Overall, these results highlight that relying solely on compatibility tests and the influence of effluents on scale formation, as observed in the soluble starch, is not sufficient to fully understand their behavior. It is likely that other molecules present in the effluents, beyond just the starchy materials, play a role in the observed effects.

Figure 10 displays the FT-IR spectra of the food effluents. The spectra exhibit a broad band in the range of 3000–3600 cm^{-1}, which corresponds to the stretching vibrations of the O–H group. The well-defined band at approximately 2930 cm^{-1} observed in spectrum (c) corresponds to the stretching vibrations of the C–H bonds. A band at 1600 cm^{-1} is present due to the angular deformation of the O–H group. Additionally, absorptions bands resulting from the bending of the CH_2 group are visible at approximately 1460 cm^{-1}, and bands at approximately 1120 cm^{-1} correspond to the stretching vibration of the C–O group. Therefore, the FTIR spectra provide evidence of the presence of several O–H groups in the starchy food effluents, which are presumably responsible for the interactions with the calcium carbonate and contribute to the inhibition of scale formation.

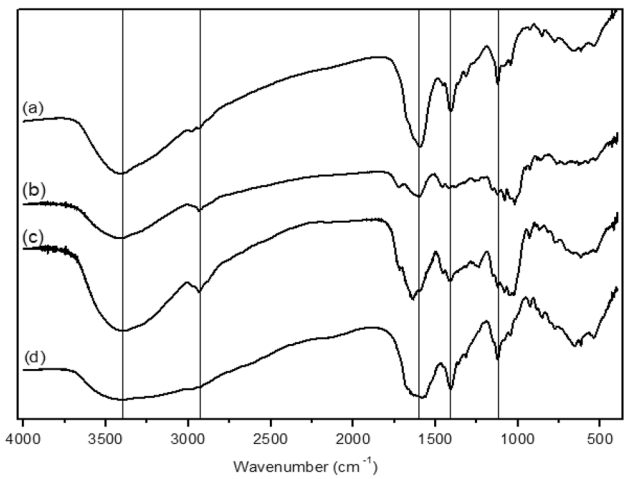

Fig. 10 The FT-IR spectra of starchy food effluents. (a) Potato peels (b) Cassava (c) Sweet Potato and (d) Potato

Considering that the food effluents primarily consist of these polyhydroxylated biopolymers, their effectiveness as calcium carbonate scale inhibitors can be attributed to similar mechanisms observed in studies of other polymeric molecules. Polymeric scale inhibitors are effective due to their ability to form complexes with inorganic salt ions, thereby preventing their precipitation. Additionally, the presence of negatively charged functional groups allows these polymers to adsorb onto the surface of the precipitates. This adsorption process helps inhibit particle agglomeration and keeps the particles suspended in the solution (Al-Roomi and Hussain 2016; Huang et al. 2019).

A study conducted in a Venezuelan oil field (Castillo et al. 2009) demonstrated that aloe vera extract can exhibit equal or even better efficiency as an inhibitor compared to commercial inhibitors. Aloe vera extract consists of various components, including amino acids, vitamins, glycosides, and minerals. Its chemical composition may vary depending on factors such as plant cultivation conditions. However, it consistently contains polysaccharides that possess carbonyl and hydroxyl groups. These functional groups have the ability to form complexes with divalent ions, which are responsible for the formation of inorganic scales. Polysaccharides present in an aqueous solution have been found to effectively control the formation of calcium carbonate crystals. This is achieved through the interaction between calcium ions and the oxygen atoms of the polysaccharide, forming coordination bonds. The large radius of calcium ions allows them to coordinate with spaced oxygen atoms, facilitating the complexation of calcium by the polysaccharides (Viloria et al. 2011).

In addition to starch, these food products are also source of proteins, carboxylic acids, other carbohydrates and fibers, minerals, vitamins, and phenolic compounds (Torres and Domínguez 2020). A study conducted by (Abdel-Gaber et al. 2011) evaluated olive leaves extract, which is rich in phenolic compounds such as oleouropein and bisphenol, as scale inhibitor. This extract was efficient in inhibiting the calcium carbonate nucleation because phenolic compounds can complex Ca^{2+} ions through their hydroxyl and carboxyl groups (Chaussemier et al. 2015). Therefore, the presence of phenolic compounds may explain the better performance of sweet potato and potato peels effluent compared to the potato effluent. The pH of the starchy food effluents could shed some light on the presence of phenolic compounds and organic acids that contribute to the inhibitory effect through carboxyl groups.

Table 5 pH of the starchy food effluents

Effluent/Molecule	pH
Potato	5.4
Potato peels	4.8
Sweet potato	4.1
Cassava	3.9

Table 6 Phenolic compounds (mg/100 g) in starchy food effluents

Phenolic compounds	Potato	Sweet potato	Potato peels	Cassava
3-CQA	ND	3.70	31.73	ND
4- CQA	ND	8.31	22.58	ND
5- CQA	ND	82.73	208.00	ND
4- FQA	ND	5.92	9.86	ND
3,4-di CQA	ND	ND	2.38	ND
3,5-di CQA	ND	0.65	24.22	ND
4,5-di CQA	ND	9.41	ND	ND
3,4-dihydroxybenzoic acid	ND	4.49	5.00	ND
Ferulic acid	ND	ND	ND	2.45

ND: not detected

Table 5 presents the pH of the effluents determined with a pH-meter SevenMulti from Mettler Toledo.

The pH of the sweet potato effluent is indeed lower than the potato effluent, suggesting the presence of a greater number of carboxyl groups. Although phenolic compounds are more concentrated in the sweet potato peel (Torres and Domínguez 2020), the potato peels effluent used in this study includes the peels of both potatoes (potato and sweet potato) and its pH is higher than the sweet potato effluent. Hence, the inhibitory performance of sweet potato effluent was better than that of potato peels effluent (Fig. 9). The presence of phenolic compounds in the starchy food effluents was confirmed using HPLC-DAD analysis, as shown in Table 6. The results of HPLC-DAD indicated the presence of ferulic acid in cassava, 3,4-dihydroxybenzoic acid, and subclasses of chlorogenic acids in sweet potato and potato peels. The chlorogenic acid subclasses identified included 3-CQA, 4-CQA, 5-CQA, 4-FQA, 3,4-diCQA, 3,5-diCQA, and 4,5-diCQA.

By examining the chemical structures of the mentioned acids (Fig. 11), it can be observed that the isomers of chlorogenic acid have a higher number of hydroxyl and carboxyl groups compared to ferulic acid. The presence of chlorogenic acid in sweet potato may be the factor that contributed to its higher inhibitory efficiency compared to the other starchy food effluents.

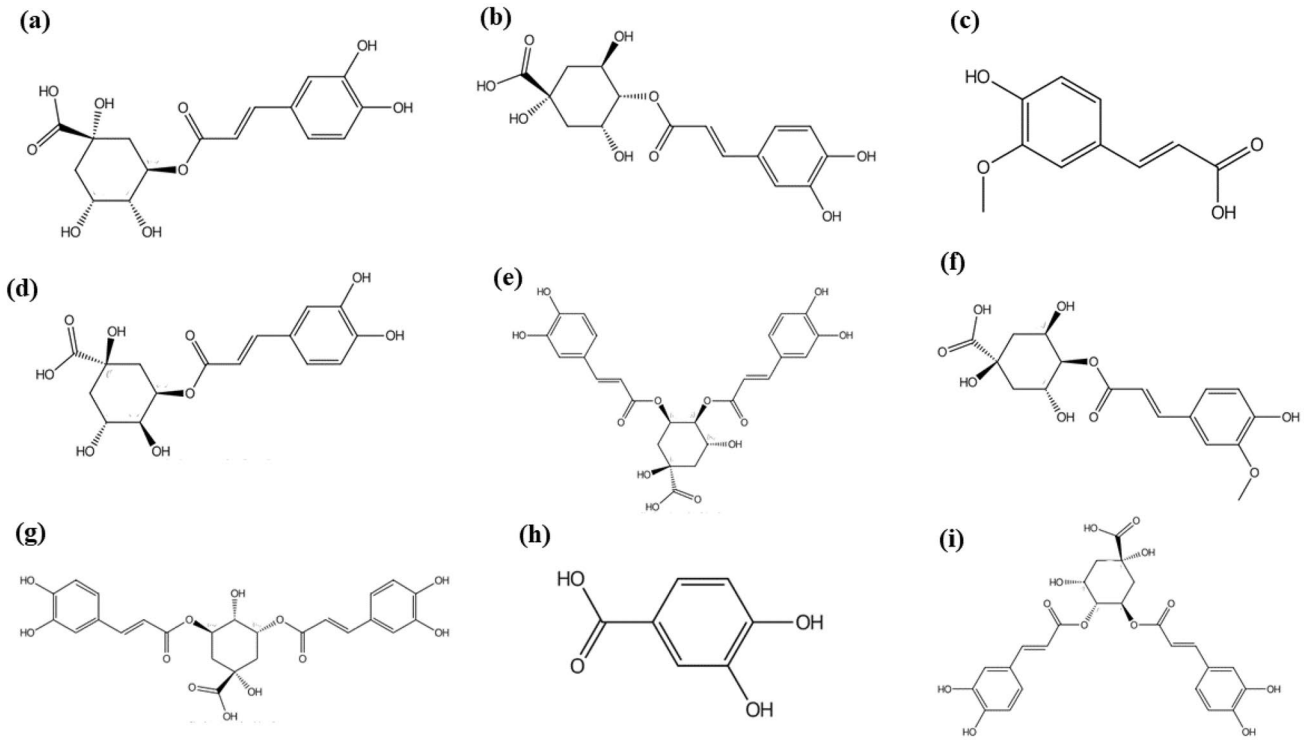

Fig. 11 Phenolic compounds present in starch food effluents. **a** 3-CQA, **b** 4-CQA, **c** ferulic acid, **d** 5- CQA, **e** 4,5-diCQA, **f** 4-FQA, **g** 3,5-di CQA, **h** 3,4-dihydroxybenzoic acid, and **i** 3,4-diCQA

Despite the higher quantity of phenolic acids in the potato peels extract compared to sweet potato, it cannot be considered an effective inhibitor because it was incompatible with brine 1 and brine 2 at a concentration of 500 mg L^{-1}. However, the sweet potato, which also contained a significant content of phenolic compounds, was compatible with brine 2 at 500 mg L^{-1} and showed good performance in the tube blocking tests, inhibiting precipitation for 1 h under these conditions (Fig. 9). In contrast, despite the pH of the cassava effluent being the lowest among all samples, only a small amount of ferulic acid was detected in it, and its inhibitory performance was the worst. This result could be explained by two reasons. Firstly, the low pH of the cassava effluent is due to the presence of ferulic acid and other organic acids or amino acids (Reis et al. 2011a). However, these compounds may have a less inhibitory effect because they possibly do not have polymeric structures. Secondly, the compatibility tests confirm the incompatibility of cassava with the two brines studied in this work, which led to secondary nucleation and the induction of scale formation.

Conclusion

Evaluating the potential of model saccharides (glucose and maltose) and polysaccharides (maltodextrin and soluble starch) to inhibit calcium carbonate scale showed the influence of the polymeric chain size on the precipitation kinetics and scale formation time. This was observed by the increase in the induction time of the precipitation experiments and by the increase in the scaling time in the tube blocking tests. However, only the soluble starch was efficient to inhibit calcium carbonate scale at a minimum concentration of 500 mg L^{-1} for the less severe brine scenario.

From the starchy food effluents evaluated in this work, only the sweet potato effluent showed to be promising to inhibit calcium carbonate scale. The potato peels effluent showed better performance than soluble starch for the more severe brine scenario. However, it is not sufficient to be considered an efficient inhibitor, and this can be attributed to its incompatibility with brine 1 and brine 2 at the concentration used for the tube blocking test. Although the potato effluent slightly influenced the scaling time, it was not efficient in inhibiting calcium carbonate scale, possibly due to the lack of phenolic compounds. Furthermore, this effluent was incompatible in both scenarios. The cassava effluent was incompatible with the brines used in this study, as scale formation occurred almost immediately in its presence. In contrast, the sweet potato is efficient to inhibit calcium carbonate scale for the less severe brine scenario, showing a better performance compared to soluble starch. These results were attributed to the presence of phenolic compounds, such as 3,4-dihydroxybenzoic acid and mainly subclasses of chlorogenic acid besides soluble starch that may also have inhibitory effects. Furthermore, sweet potato was compatible in brine 2 for 500 mg L^{-1}.

The sweet potato effluent demonstrated potential as an inhibitor calcium carbonate scale. However, further studies are necessary to investigate and enhance its performance. These studies should be focused on determining the polymer chain size of the polysaccharides present in the effluent, as this study suggest that it has an effect on calcium carbonate precipitation kinetics. Additionally, other studies should be conducted to evaluate specific criteria that a commercial scale inhibitor must meet, such as thermal resistance, effective performance at low concentrations, resistance to pH variations, strong affinity with other inorganic salts, water solubility, and cost-effectiveness.

The findings of this study highlight the significance of exploring other starchy food effluents that, as the sweet potato, could be eventually used as scale inhibitors. Thus, the starchy effluents may become an abundant and cost-effective source of biodegradable molecules for the development of green scale inhibitors.

Acknowledgements The Human Resources Program of the National Agency of Petroleum, Natural Gas, and Biofuels of Brazil PRH-ANP (in Portuguese) supported this research with funds from the investment of oil companies qualified in the R&DI Clause of ANP Resolution 50/2015. The authors thank to the National Center of Structural Biology and Bioimage of the Federal University of Rio de Janeiro CENABIO/UFRJ (in Portuguese) for providing the infrastructure to perform the scanning electron microscopy analysis. The authors show gratitude to the SENAI Institute of innovation in fibers and biosynthetics ISI B&F SENAI/CETIQT (in Portuguese) for the support with the X-ray diffraction and Raman spectroscopy analysis. The authors also are grateful to the Microbial Biotechnology Laboratory, LabBim/IQ-UFRJ, for facilitating the infrastructure to freeze-dry the starchy food effluents.

Declarations

Conflict of interest On behalf of all authors, the corresponding author states that there is no conflict of interest.

References

Abdel-Gaber AM, Abd-El-Nabey BA, Khamis E, Abd-El-Khalek DE (2011) A natural extract as scale and corrosion inhibitor for steel surface in brine solution. Desalination 278:337–342. https://doi.org/10.1016/j.desal.2011.05.048

Al-Roomi YM, Hussain KF (2016) Potential kinetic model for scaling and scale inhibition mechanism. Desalination 393:186–195. https://doi.org/10.1016/j.desal.2015.07.025

Anastácio A, Silva R, Carvalho IS (2016) Phenolics extraction from sweet potato peels: modelling and optimization by response surface modelling and artificial neural network. J Food Sci Technol 53:4117–4125. https://doi.org/10.1007/s13197-016-2354-1

Bergel BF, Dias Osorio S, da Luz LM, Santana RMC (2018) Effects of hydrophobized starches on thermoplastic starch foams made

from potato starch. Carbohydr Polym 200:106–114. https://doi.org/10.1016/j.carbpol.2018.07.047
Bisatto R, Picoli VM, Petzhold CL (2022) Evaluation of different polymeric scale inhibitors for oilfield application. J Pet Sci Eng 213:110331. https://doi.org/10.1016/j.petrol.2022.110331
Castillo LA, Torin EV, Garcia JA et al (2009) New product for inhibition of calcium carbonate scale in natural gas and oil facilities based on aloe vera: application in venezuelan oilfields. SPE Lat Am Caribb Pet Eng Conf Proc 3:1456–1463. https://doi.org/10.2118/123007-ms
Chaussemier M, Pourmohtasham E, Gelus D et al (2015) State of art of natural inhibitors of calcium carbonate scaling. A review article. Desalination 356:47–55. https://doi.org/10.1016/j.desal.2014.10.014
Costa AG, Souza S, Alisson F et al (2021) Characterization of cassava wastewaters from the processing of different cassava cultivars. Sci J Environ Sci Biotechnol 7:39–47
da Costa IVL, Rochedo P, Império M et al (2016) Geo.: gas production in Offshore Reservoirs in Brazil's Pre-salt Region. In: Grammelis P (ed) Energy,transportation and global warming. Springer, Basel, Switzerland, pp 617–629
da Rosa KRSA, Fontes RA, do Rosário FF et al (2020) Improved protocol for scale inhibitor evaluation: A meaningful step on scale management. Offshore Technol Conf Bras 2019, OTCB 2019. https://doi.org/10.4043/29683-ms
Elkholy AE, El-Taib Heakal F, Rashad AM, Zakaria K (2018) Monte Carlo simulation for guar and xanthan gums as green scale inhibitors. J Pet Sci Eng 166:263–273. https://doi.org/10.1016/j.petrol.2018.03.019
Ferreira VF, Rocha DR da, de Silva F (2009) C Pontecialidade e oportunidades na química da sacarose e outras açucares. Quim Nova 32:623–638
Hasson D, Shemer H, Sher A (2011) State of the art of friendly green scale control inhibitors: a review article. Ind Eng Chem Res 50:7601–7607. https://doi.org/10.1021/ie200370v
Huang H, Yao Q, Jiao Q et al (2019) Polyepoxysuccinic acid with hyper-branched structure as an environmentally friendly scale inhibitor and its scale inhibition mechanism. J Saudi Chem Soc 23:61–74. https://doi.org/10.1016/j.jscs.2018.04.003
Jafar Mazumder MA (2020) A review of green scale inhibitors: process, types, mechanism and properties. Coatings 10:1–29. https://doi.org/10.3390/coatings10100928
Jensen MK, Kelland MA (2012) A new class of hyperbranched polymeric scale inhibitors. J Pet Sci Eng 94–95:66–72. https://doi.org/10.1016/j.petrol.2012.06.025
Kamal MS, Hussein I, Mahmoud M et al (2018) Oilfield scale formation and chemical removal: a review. J Pet Sci Eng 171:127–139. https://doi.org/10.1016/j.petrol.2018.07.037
Kartnaller V, Venâncio F, do Rosário FF, Cajaiba J (2018) Application of multiple regression and design of experiments for modelling the effect of monoethylene glycol in the calcium carbonate scaling process. Molecules 23:1–12. https://doi.org/10.3390/molecules23040860
Kumar S, Naiya TK, Kumar T (2018) Developments in oilfield scale handling towards green technology-A review. J Pet Sci Eng 169:428–444. https://doi.org/10.1016/j.petrol.2018.05.068
Li J, Tang M, Ye Z et al (2017) Scale formation and control in oil and gas fields: a review. J Dispers Sci Technol 38:661–670. https://doi.org/10.1080/01932691.2016.1185953
Liu LX, He AJ (2014) Research progress of scale inhibition mechanism. Adv Mater Res 955–959:2411–2414. https://doi.org/10.4028/www.scientific.net/AMR.955-959.2411
Macedo RGMD, Marques A, Paulucci do NLCS et al (2019) Water-soluble carboxymethylchitosan as green scale inhibitor in oil wells. Carbohydr Polym 215:137–142. https://doi.org/10.1016/j.carbpol.2019.03.082
MacNeill GJ, Mehrpouyan S, Minow MAA, Patterson JA, Tetlow IJ, Emes MJ (2017) Starch as a source, starch as a sink: the bifunctional role of starch in carbon allocation. J Exp Bot 68(16):4433–4453. https://doi.org/10.1093/jxb/erx291
Manoli F, Dalas E (2000) Spontaneous precipitation of calcium carbonate in the presence of ethanol, isopropanol and diethylene glycol. J Cryst Growth 218:359–364. https://doi.org/10.1016/S0022-0248(00)00560-1
Martinod A, Neville A, Euvrad M, Sorbie K (2009) Electrodeposition of a calcareous layer: Effects of green inhibitors. Chem Eng Sci 64:2413–2421. https://doi.org/10.1016/j.ces.2009.01.024
Meldrum FC (2003) Calcium carbonate in biomineralisation and biomimetic chemistry. Int Mater Rev 48:187–224. https://doi.org/10.1179/095066003225005836
Mironescu M (2011) Investigations on wastewaters at potato processing and starch recovery and characterisation. J Agroaliment Process Technol 17:134–138
Moorthy SN (2002) Physicochemical and Functional Properties of Tropical Tuber Starches: A Review. Starch/Stärke, 54: 559–592. https://doi.org/10.1002/1521-379X(200212)54:12<559::AID-STAR2222559>3.0.CO;2-F
Patterson AL (1939) The scherrer formula for X-ray particle size determination. Phys Rev 56:978–982. https://doi.org/10.1103/PhysRev.56.978
Rao A, Berg JK, Kellermeier M, Gebauer D (2014) Sweet on biomineralization: effects of carbohydrates on the early stages of calcium carbonate crystallization. Eur J Mineral 26:537–552. https://doi.org/10.1127/0935-1221/2014/0026-2379
Reis IAO, Santos RM, Souza JF et al (2011a) Characterization of flour obtained from waste of cassava minimally processed. Sci Plena 7:1–11
Reis MIP, Da Silva FDC, Romeiro GA et al (2011b) Mineral scale deposition in surfaces: problems and opportunities in the oil industry. Rev Virtual Quim 3:2–13. https://doi.org/10.5935/1984-6835.20110002
Schenk AS, Zope H, Kim YY et al (2012) Polymer-induced liquid precursor (PILP) phases of calcium carbonate formed in the presence of synthetic acidic polypeptides - relevance to biomineralization. Faraday Discuss 159:327–344. https://doi.org/10.1039/c2fd20063e
Sebastiani F, Wolf SLP, Born B et al (2017) Water Dynamics from THz Spectroscopy reveal the locus of a liquid–liquid Binodal Limit in Aqueous CaCO3Solutions. Angew Chemie - Int Ed 56:490–495. https://doi.org/10.1002/anie.201610554
Torres MD, Domínguez H (2020) Valorisation of potato wastes. Int J Food Sci Technol 55:2296–2304. https://doi.org/10.1111/ijfs.14228
Venancio F, Rosário FF, Cajaiba J (2018) Use of a dynamic system and reflectance measurements to assess the impact of monoethylene glycol on calcium carbonate scale. J Pet Sci Eng 165:581–585. https://doi.org/10.1016/j.petrol.2018.02.064
Viloria A, Castillo L, García JA et al (2011) Process using aloe for inhibiting scale. 4
Wang Y, Li Y, Zhang H (2017) A soluble starch synthase I gene, IbSSI, alters the content, composition, granule size and structure of starch in transgenic sweet potato. Sci Rep 7:2315. https://doi.org/10.1038/s41598-017-02481-x
Wang H, Hu J, Yang Z et al (2021) The study of a highly efficient and environment-friendly scale inhibitor for calcium carbonate scale in oil fields. Petroleum 7:325–334. https://doi.org/10.1016/j.petlm.2021.01.005
Zakyatul U, Khaled H, Elraies A et al (2022) A review: the utilization potency of biopolymer as an eco – friendly scale inhibitors. J Pet Explor Prod Technol 12:1075–1094. https://doi.org/10.1007/s13202-021-01370-4